Proceedings of IMECE04
2004 ASME International Mechanical Engineering Congress and Exposition
November 13-20, 2004, Anaheim, California USA

IMECE2004-61638

Vehicle Handling and Stability Enhancement with Active Steering Control Systems

Shih-Ken Chen
William C. Lin
Yuen-Kwok Steve Chin
General Motors Corp.

Xiaodi Kang
Quantech Global Service

Keywords: Front-Wheel Steering, Active front Steering, Rear-Wheel Steering, Four-wheel Steering

ABSTRACT

This paper presents an analysis and comparison of a vehicle with active front steering and rear-wheel steering. Based on linear analysis of base vehicle characteristics under varying speed and road surfaces, desirable vehicle response characteristics are presented and a set of performance matrices for active steering systems is formulated. Using pole-placement approach, controllability issues under active front wheel steering and rear- wheel steering controls are discussed. A frequency response optimization approach is then used to design the closed-loop controllers.

INTRODUCTION

Active steering systems have been extensively investigated in the past two decades as a new approach for enhancing vehicle handling and stability characteristics. Several steering control systems, including rear-wheel steering (RWS) or four wheel steering (4WS), active front steering (AFS), and all wheel steering (AWS) have been reported [1-2]. However, it appears that there is relatively little published work explicitly dealing with the fundamental aspects of active steering system design and analysis, particularly, desirable vehicle handling characteristics, criteria for steering system design and assessment, control authority comparison, advantages and drawbacks of different steering control approaches and mechanisms.

This paper presents an analysis and comparison of vehicle performance when equipped with AFS and RWS. Based on analysis of the base vehicle characteristics under varying speed and surfaces, desirable vehicle response characteristics are described and a set of performance matrices for active steering system design and evaluation is formulated. Based on the pole-placement approach, controllability issues for front-wheel steering and rear-wheel steering control are discussed and a frequency response optimization approach is further proposed to design the closed-loop controllers. Simulations are also carried out to verify the analysis and to evaluate the controller performance under different maneuvers.

NOMENCLATURE

a	distance from vehicle CG to front axle
b	distance from vehicle CG to rear axle
C_f	front cornering stiffness
C_r	rear cornering stiffness
e	distance of disturbance force from c.g.
F_{yf}	front tire lateral force
F_{yr}	rear tire lateral force
F_d	side disturbance force
g	gravitational acceleration
G_{vd}	desired sideslip transfer function
G_{vc0}	sideslip steady-state gain under steering control
G_{vd0}	desired sideslip steady-state gain
G_{vs0}	base vehicle sideslip steady-state gain
G_{rd}	desired yaw-rate transfer function
G_{rc0}	yaw-rate steady-state gain under steering control
G_{rd0}	desired yaw-rate steady-state gain
G_{rs0}	base vehicle yaw-rate steady-state gain
I	identity matrix
I_z	vehicle yaw moment of inertia
J	cost function
k_ψ	radius of gyration
K_{fsp}	AFS sideslip control P-gain
K_{frp}	AFS yaw-rate control P-gain
K_{rsd}	RWS sideslip control D-gain
K_{rsp}	RWS sideslip control P-gain
K_{rrd}	RWS yaw-rate control D-gain

K_{rrp}	RWS yaw-rate control P-gain
M	vehicle mass
n_{st}	front steering gear ratio
r	yaw rate
r_d	desired yaw rate
r_{max}	maximum achievable yaw rate
s	Laplace trasnferm
v_x	vehicle forward speed
v_{xc}	critical vehicle forward speed
v_y	vehicle sideslip
v_{yd}	desired vehicle sideslip
x	state matrix
Z_{rd}	yaw-rate transfer function zero
Z_{rs}	base vehicle yaw-rate transfer function zero
Z_{vd}	sideslip transfer function zero
Z_{vs}	base vehicle sideslip transfer function zero
δ_f	front wheel steering angle
δ_{fd}	desired front wheel steering angle
δ_r	rear wheel steering angle
δ_{rb}	closed-loop RWS control
δ_{rf}	open-loop RWS control
μ	surface friction coefficient
θ_{HW}	driver hand-wheel angle
ω_0	base vehicle natural frequency
ω_d	desired natural frequency
ω_n	natural frequency
ζ	damping ratio
ζ_0	base vehicle damping ratio
ζ_d	desired damping ratio
λ	weighting coefficient

A FOUR-WHEEL-STEERING VEHICLE MODEL

For the analysis, the well known linear bicycle model is adopted. Referring to Figure 1, for a four-wheel-steering (4WS) vehicle having yaw-plane motion with constant forward speed v_x, the equations of motion using vehicle-body fixed coordinate system *xoy* are given by:

$$\begin{aligned} M(\dot{v}_y + v_x r) &= F_{yf}\cos\delta_f + F_{yr}\cos\delta_r + F_d \\ I_z\dot{r} &= aF_{yf}\cos\delta_f - bF_{yr}\cos\delta_r + eF_d \end{aligned} \tag{1}$$

Assuming small wheel angles and a simple linear tire model and substituting the cornering forces (F_{yf} and F_{yr}) as linear functions of cornering stiffness and tire slip angles yields the following dynamic equations of motion:

$$\begin{bmatrix} \dot{v}_y \\ \dot{r} \end{bmatrix} = \begin{bmatrix} a_{11} & a_{12} \\ a_{21} & a_{22} \end{bmatrix} \begin{bmatrix} v_y \\ r \end{bmatrix} + \begin{bmatrix} b_{11} \\ b_{21} \end{bmatrix} \delta_f + \begin{bmatrix} b_{12} \\ b_{22} \end{bmatrix} \delta_r + \begin{bmatrix} \frac{1}{M} \\ \frac{e}{I_z} \end{bmatrix} F_d \tag{2}$$

where the system coefficients, a_{ij} and b_{ij}, are functions of vehicle parameters, as listed in the Appendix.

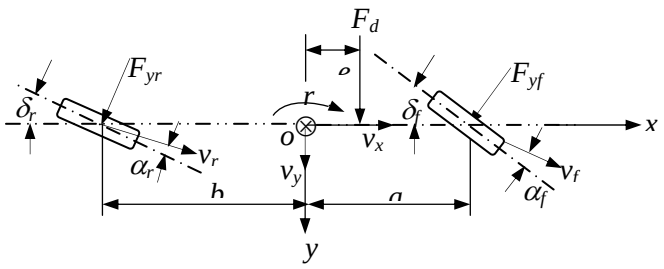

Figure 1: A two-DOF 4WS bicycle vehicle model

The matrix representation of the four-wheel-steering vehicle system is written as:

$$\dot{x} = Ax + B_f\delta_f + B_r\delta_r \tag{3}$$

where x consists of v_y and r, A represents the state matrix, and the input vectors B_f and B_r are defined by:

$$B_f = \begin{bmatrix} b_{11} \\ b_{21} \end{bmatrix}, \quad B_r = \begin{bmatrix} b_{12} \\ b_{22} \end{bmatrix} \tag{4}$$

The state equations of a conventional front-wheel steering vehicle can be readily obtained by setting the rear wheel steering angle to zero in equation (3), given by:

$$\dot{x} = Ax + B_f\delta_f \tag{5}$$

The natural frequency (ω_n) and damping ratio (ζ) of the base vehicle system can be directly derived from the system matrix A in equation (3) or equation (5), expressed as

$$\begin{cases} \omega_n = \sqrt{a_{11}a_{22} - a_{12}a_{21}} \\ \zeta = \dfrac{a_{11} + a_{22}}{2\omega_n} \end{cases} \tag{6}$$

OPEN-LOOP VEHICLE CHARACTERISTICS

Vehicle natural frequency and damping ratio variations

From the system matrix A, the natural frequency and damping ratio of the vehicle yaw-plane motion can be evaluated. Figure 2 shows that the natural frequency and the damping ratio both gets smaller as the vehicle speed increases and the surface friction decreases. The results demonstrate that surface friction coefficient affects both the natural frequency and the damping ratio considerably. It also shows that vehicle speeds mainly influence the damping ratio, especially in the high speed region. Furthermore, while the damping ratio decreases rapidly with increasing vehicle speeds, the natural frequency remains nearly constant at relatively high speeds regardless of surface conditions. The damping ratio, however, becomes very low at high speed.

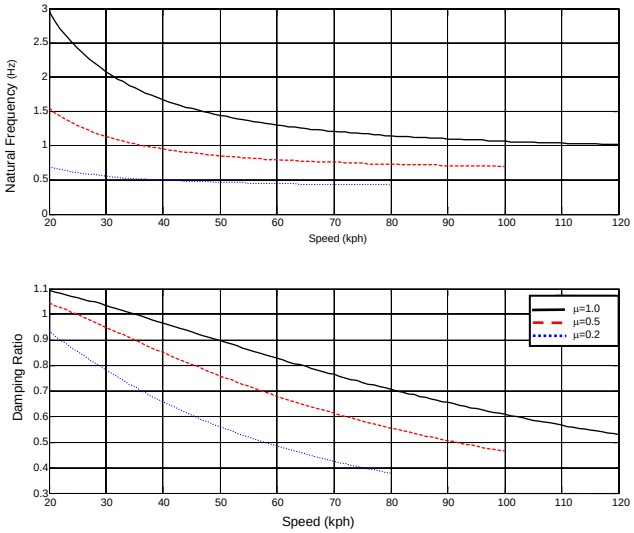

Figure 2: Yaw Natural frequency and damping ratio of the base vehicle as functions of vehicle speed on different surfaces

Comparison of vehicle responses under FWS and RWS inputs

Figure 3 presents a comparison of vehicle sideslip and yaw rate frequency and step-input time responses under both FWS and RWS inputs at two different speeds on a high-co surface (μ=1.0), while Figure 4 presents a similar comparison on medium-co (μ=0.5) surface. It should be pointed out that to facilitate yaw-rate comparison with FWS, the RWS input is assumed to be the negative of the FWS input magnitude so that they generate yaw rate with the same sign. This would not affect any analysis results using a bicycle model.

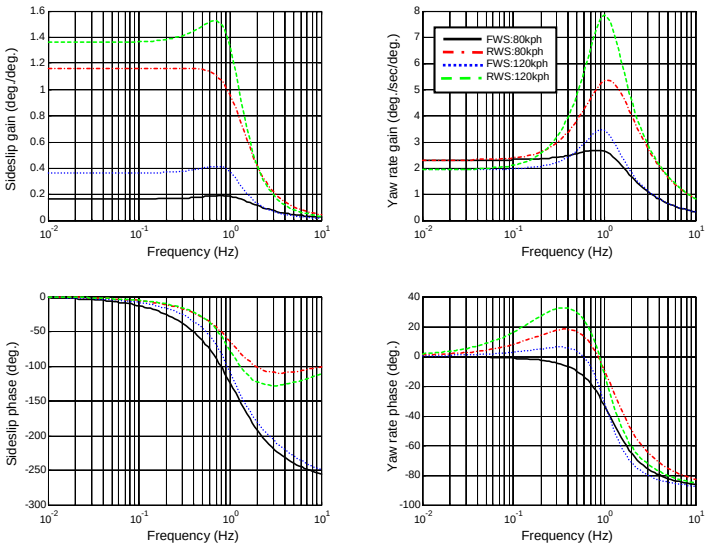

Figure 3: Sideslip and yaw rate response to FWS and RWS (high-co, μ=1.0)

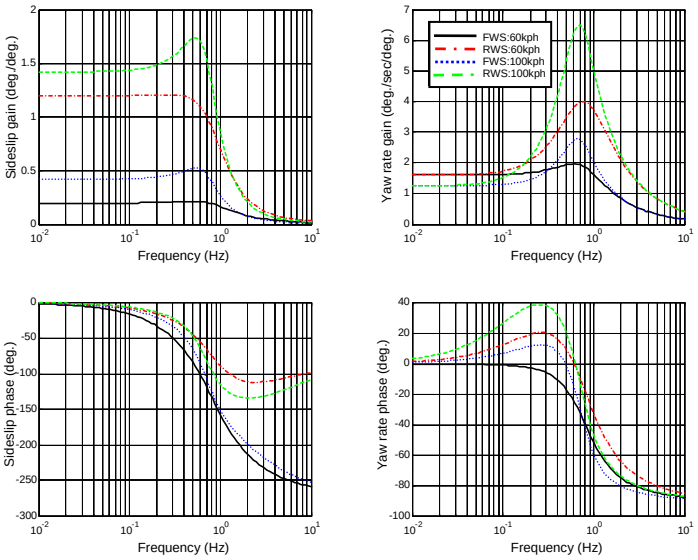

Figure 4: Sideslip and yaw rate response to FWS and RWS (low-co, μ=0.5)

Figures 3 and 4 demonstrate that both steering inputs yield the same steady-state responses in vehicle yaw rate and tire slip angles, while the vehicle is more responsive to RWS than FWS in its side-slip velocity response. In terms of transient response, RWS reveals higher responsiveness and smaller phase delay, but it leads to considerably larger resonant peak. Under both steering inputs, however, sideslip velocity exhibits considerably lower resonant peak ratio (the ratio of the maximum frequency response magnitude and the dc-gain) than yaw rate.

Figure 5 summarizes the vehicle frequency response characteristics as a function of vehicle speed under two typical surfaces. Figure 6 demonstrates that yaw rate steady-state gains under both steering inputs initially increase as the vehicle speed increases, reach their respective maximum values, and then gradually decrease as the vehicle speed further increases, indicative of an understeer vehicle. The steady-state sideslip gain under RWS increases monotonically with rising vehicle speeds while the side-slip gain under FWS crosses zero at a certain speed and then increases in magnitude. Figure 5 further shows that the vehicle yaw rate bandwidth and resonant peak ratios under RWS are significantly higher than those under FWS, regardless of vehicle speed and surface condition
From the above FWS analysis results, it is observed that the base vehicle sideslip, yaw rate resonant-peak ratio become increasingly larger with increasing speed. The yaw rate shows a fast but oscillatory response with significant overshoot, especially at high speed and on low-co surfaces.

Therefore, with AFS under more challenging maneuvers (high speed, low-co, or both), the reduced effectiveness of driver steering control due to increased sideslip and slower response

for the vehicle yawing motion to the driver steering input may become significant and the oscillation of the yawing motion becomes so excessive that the driver may experience a certain difficulty in controlling the vehicle along the intended path. This difficulty increases with increasing vehicle speed and reducing surface friction. This needs to be overcome to ensure desirable and consistent handling characteristics for the driver.

It is also observed that while FWS and RWS yield the same yaw rate steady-state gain, RWS produces significantly larger sideslip steady-state gain, especially at relatively high speeds. Figure 6 summarize the steady-state gains for FWS and RWS under different control input angle. It illustrates the effectiveness of FWS and RWS in influencing the vehicle steady-state response at 100kph for different input wheel angle. The comparison suggests that RWS is considerably more effective in generating vehicle sideslip, especially when the vehicle operation speed goes through a considerable range and thus can enhance vehicle stability better than AFS. However, figure 5 also shows that RWS yields considerably higher resonant peak ratio than FWS, suggesting that the damping of RWS feedback control requires additional attention in its design.

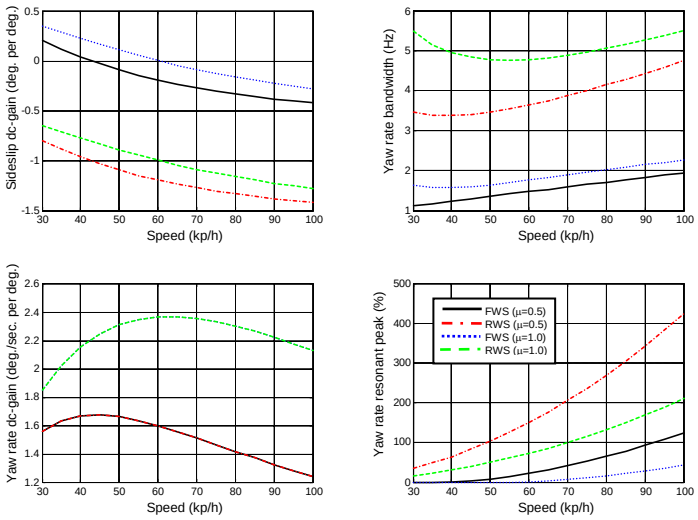

Figure 5: Vehicle frequency response characteristics under FWS and RWS inputs

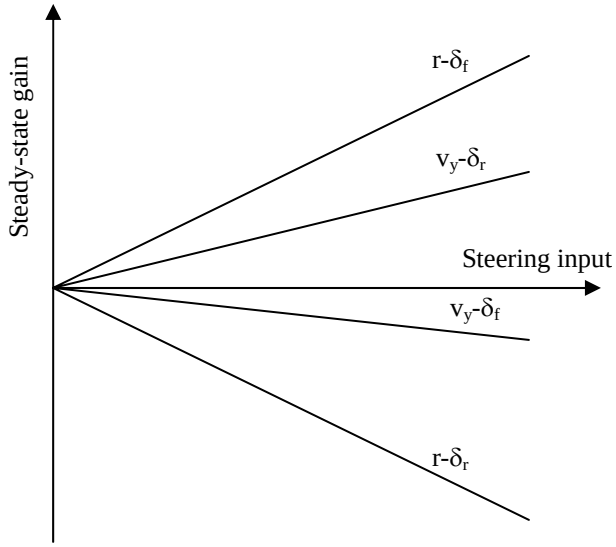

Figure 6: Control authority of FWS and RWS inputs

ACTIVE STEERING SYSTEM DESIGN

Control System Configuration

The active steering controller design is carried out based on the linear vehicle dynamics model described in the previous section. Under both open-loop and closed-loop controls, the block diagram of a yaw-rate and sideslip feedback 4WS control system is illustrated in Figure 7. In the case of active rear wheel steering, only RWS control portion is enabled, while in the case of active front wheel steering, only AFS control portion is activated.

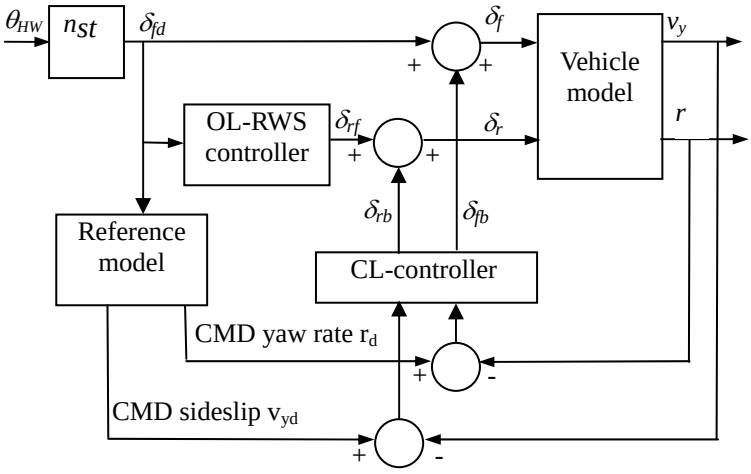

Figure 7: A 4WS control configuration

The closed-loop vehicle system state equation under both front and rear wheel steering control.

$$\dot{x} = (A - B_f K_{fp} - B_r K_{rp})x + (B_f + B_r K_f)\delta_f + (B_f K_{fp} + B_r K_{rp})x_d \quad (7)$$

where x_d denotes the desirable/reference vehicle state, $x_d=[v_{yd}, r_d]^t$, $K_{fp}=[K_{fsp}, K_{frp}]$, and $K_{rp}=[K_{rsp}, K_{rrp}]$,

If adding derivative control, the closed-loop system state equation becomes:

$$(I + B_f K_{fd} + B_r K_{rd})\dot{x} = (A - B_f K_{fp} - B_r K_{rp})x + (B_f + B_r K_f)\delta_{fd} + (B_f K_{fp} + B_r K_{rp})x_d + (B_f K_{fd} + B_r K_{rd})\dot{x}_d \quad (8)$$

where $K_{rd}=[K_{rsd}, K_{rrd}]$ denotes sideslip and yaw-rate D gain, and $\dot{x}_d = [\dot{v}_{yd}, r_d]^t$ denotes desirable rate of vehicle states.

Desirable Vehicle Response and Control Design Criteria

Assuming the desirable sideslip velocity and yaw-rate transfer function vector to be G_d, which can be generally expressed as:

$$\begin{bmatrix} G_{vd} \\ G_{rd} \end{bmatrix} = \frac{\omega_d^2}{s^2 + 2\zeta_d \omega_d s + \omega_d^2} \begin{bmatrix} G_{vd0}(1 - \frac{s}{Z_{vd}}) \\ G_{rd0}(1 - \frac{s}{Z_{rd}}) \end{bmatrix} \quad (9)$$

The reference parameters in the above desired transfer function or reference model can be intuitively derived based on those of the base FWS vehicle under a relatively high-coefficient surface (i.e., a targeting surface) condition and considerations of the following preferable vehicle response characteristics [1, 2, 6] to achieve enhanced vehicle response quality. Specifically, in time domain, the following are representative of improved handling response and directional stability characteristics:

- Steady-state: minimal body sideslip to enhance handling stability (near linear handling characteristics and thus more predictable), and consistent yaw rate gain to driver steering input to maintain acceptable steering sensitivity of the vehicle.
- Transient characteristics: short rise time and
- Settling time for step steering, and minimal percent overshoot/oscillatory.

In frequency domain, it is desirable that:

- The transfer function of yaw rate to driver steering input reveals considerably flat frequency characteristics to enlarge yaw rate bandwidth and yawing responsiveness.
- Minimal resonant-peak ratio to enhance system damping.
- Minimal yaw-rate phase delay, and minimal phase lag between yaw rate and lateral acceleration (equivalent to minimizing the maximum body sideslip), since an advance in the phase of both yaw rate and lateral acceleration dramatically improves vehicle controllability/followability [1].

The reasonable sideslip steady-state gain can be intuitively determined based on that of the base FWS vehicle on high-co and sideslip limitation considerations to ensure adequate control authority for the driver and nearly linear vehicle characteristics with which a normal driver is familiar. As has been previously reported [7], large sideslip reduces the achievable yaw moment and cornering forces, causing nonlinear vehicle behaviors. In addition, it is observed that a normal driver usually drives under situations when vehicle sideslip angle is quite small (less than 2 degrees).

The desirable and yet feasible yaw-rate steady-state gain is to be determined based on that of the base FWS vehicle to maintain consistent steering sensitivity and the maximum achievable yaw rate, which is limited by the operating surface and vehicle speed:

$$r_{max} = \frac{g\mu}{v_x} \quad (10)$$

The above desired steady-state and transient response requirements are then translated into the desirable transfer function vector for controller design.

Based on the above description, several criteria for the closed-loop steering control design and evaluation are further formulated as follows:

- Regulation of vehicle body sideslip to ensure that vehicle sideslip is within a reasonable range while trying to preserve the yaw-rate gain.
- Enhancement of vehicle transient response quality, such as damping characteristics, responsiveness and phase delay (increase of yaw-rate bandwidth and reduction of yaw-rate overshoot and phase delay).
- Consideration of tire cornering force saturation and reasonable steering control ranges.

State Feedback and Controllability Issues

The feedback gains in the closed-loop state equations (equations (7) and (8)) can be determined in many ways to achieve different design requirements. For a preliminary analysis, the closed-loop feedback gains can be designed to simply modify the eigenvalues of the vehicle yawing motion for enhanced stability and handling response characteristics, i.e., more responsive and damped, using the pole-placement approach. For a standard second-order system, the design specifications are expressed in terms of the desired natural frequency (denoted by ω_d) and desired damping ratio (denoted by ζ_d).

Based on the closed-loop system state matrix in equation (7), a general analytical expression for state feedback gains (for AFS and RWS, respectively) in terms of base-vehicle transfer

functions is derived as follows:

$$\begin{bmatrix} K_{sp} \\ K_{rp} \end{bmatrix} = \begin{bmatrix} \frac{G_{vs0}}{Z_{vs}} & \frac{G_{rs0}}{Z_{rs}} \\ G_{vs0} & G_{rs0} \end{bmatrix}^{-1} \begin{bmatrix} \frac{2\zeta_d \omega_d - 2\zeta_0 \omega_0}{\omega_0^2} \\ (\frac{\omega_d}{\omega_0})^2 - 1 \end{bmatrix} \quad (11)$$

Eq. (11) demonstrates that the state-feedback gains (K_{sp} and K_{rp}) are functions of base- vehicle static gains, transmission zeros, and natural frequencies and damping ratios of the base and desirable/target vehicles. The first term on the right-hand side indicates possible gain discontinuity when the matrix becomes singular at certain speeds. This possible discontinuity is entirely dependent on the relationship among static gains and zeros of sideslip and yaw rate transfer functions.

Under state feedback front wheel steering control, the possible vehicle speed leading to zero denominator in equation (11) is derived as:

$$v_{xc} = \sqrt{\frac{C_r}{M}\frac{(a+b)}{a^2}(ab - k_\psi^2)} \quad (12)$$

where k_ψ is the radius of gyration (I_z/M, equivalent point of mass concentration relative to vehicle c.g.) of the vehicle mass in the yaw axis.

Eq. (12) indicates that when k_ψ is greater than the geometric mean of c.g. location relative to the two axles ($\sqrt{ab}$) the system is always controllable [8].

Under rear-wheel-steering control, the possible vehicle speed leading to zero denominator in equation (12) is derived as:

$$v_{xc} = \sqrt{\frac{C_f}{M}\frac{(a+b)}{b^2}(k_\psi^2 - ab)} \quad (13)$$

Eq. (13) indicates that, contrary to front wheel steering control case, when k_ψ is less than $\sqrt{ab}$ the system is controllable at a certain speed.

The pole-placement design is based on an ideal second-order system, and can yield improved vehicle performance, especially in terms of vehicle yawing responsiveness and damping characteristics. In addition, it can reveal insights regarding system controllability under state feedback control. It, however, can not ensure that the gain design is optimal in terms of vehicle response characteristics. In the existence of finite transfer-function zeros, it is difficult to know exactly where the system poles should be placed to ensure desirable vehicle performance. This is attributed to the fact that the open-loop control and pole-zero interactions can not be incorporated in the pole-placement design.

Control Design using Numerical Optimization

A multi-parameter optimization is proposed to design the closed-loop steering control in this section. The design variables are the adjustable feedback gains and the objective can be formulated as a performance index or cost function to enhance vehicle stability and handling response characteristics.

Many optimization functions can be formulated to determine the active steering controller gains. In this paper, the closed-loop control design is mainly based on minimizing the difference between the desired vehicle responses and those of the closed-loop controlled vehicle, namely, sideslip and yaw-rate tracking errors. Therefore, an equivalent optimization problem is defined as:

$$\text{Min } J = \lambda(G_{vd0} - G_{vc0})^2 + (1-\lambda)(G_{rd0} - G_{rc0})^2 \quad (14)$$

where λ is a weighting coefficient to reflect steering control design preference, while G_{vc0} and G_{rc0} represent sideslip and yaw rate dc-gains of the vehicle under closed-loop steering control.

The optimization assumes the following frequency and time-domain constraints:

- Sideslip resonant peak is not greater than a pre-set value.
- Maximum tire slip angle under typical severe maneuvers is not greater than the saturation slip angle.
- Yaw rate resonant peak ratio is not greater than a pre-set magnitude.
- Yaw rate bandwidth is not less than a reference value.
- Yaw rate phase delays under typical/high steering frequencies (0.5~2 Hz) are not greater than the reference values.
- Active steering angles due to either state or state errors under typical/severe steering maneuvers are in a reasonable range (for example, corrective steering angles can be assumed to be in the range of -1.5 to 1.5 degrees)

The reference parameters in the above frequency measure constraints are intuitively determined by analysis of the desirable vehicle response characteristics and consideration of vehicle response property on high-co surfaces, while the saturation or critical tire slip angles are obtained from tire cornering force characteristics.

Figure 8 presents comparisons of the frequency response of the vehicle under closed-loop AFS control with those of the base vehicle at75 kp/h. The closed-loop ASF control is obtained by setting the upper limits of sideslip angle gain to 0.25, based on base vehicle sideslip response on high-co. Again, the results clearly show that regulation of sideslip and enhancement of yaw-rate transient response quality lead to correspondingly

reduced static yaw-rate gain. So there should be an appropriate trade-off between vehicle sideslip and yaw rate (i.e., stability vs. steerability) based on the particular driver skill and preference. Figure 9 presents the frequency response of the vehicle under RWS control with those of the base vehicle under the same condition.

Comparison of Figures 8 and 9 demonstrates that RWS can achieve better performance on both side-slip reduction and yaw-rate tracking than AFS.

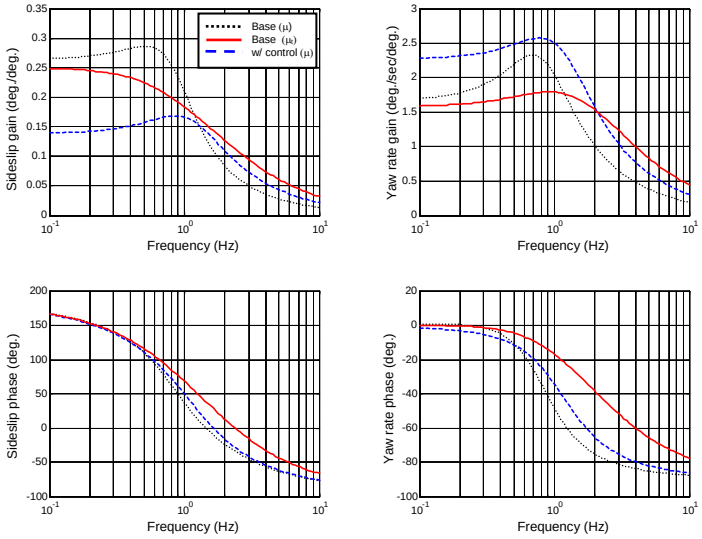

Figure 8: Frequency response of the base and AFS-controlled vehicles

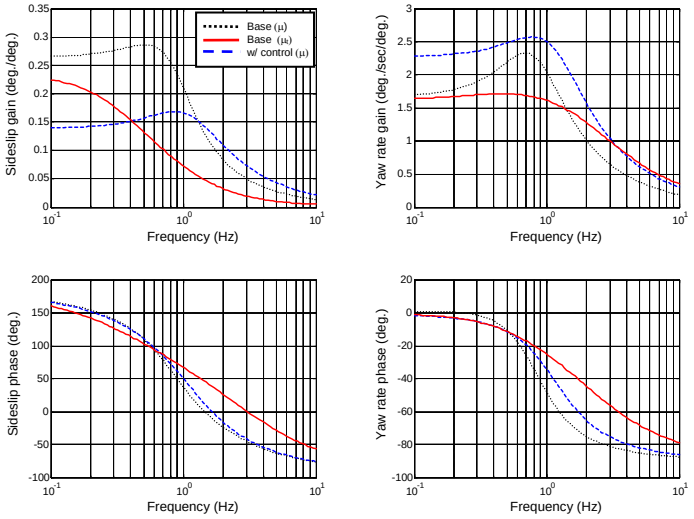

Figure 9: Frequency response of the base and RWS controlled vehicles

SIMULATION

To validate the proposed active steering control, nonlinear full vehicle model simulations are performed. This section describes some evaluation results of control performance using AFS and RWS in comparison to the base vehicle performance.

Fig. 10 shows the vehicle responses for emergency double-lane-change maneuver on packed snow surface. For this maneuver, the vehicle is driving at constant speed of 75 kph and the driver first applies a large quick steering wheel input to initiate a lane change followed by a similar, but opposite in direction, steering wheel input to return the vehicle to the original lane. The comparison shows that both AFS and RWS can improve the vehicle stability and RWS is more effective in controlling the side-slip velocity.

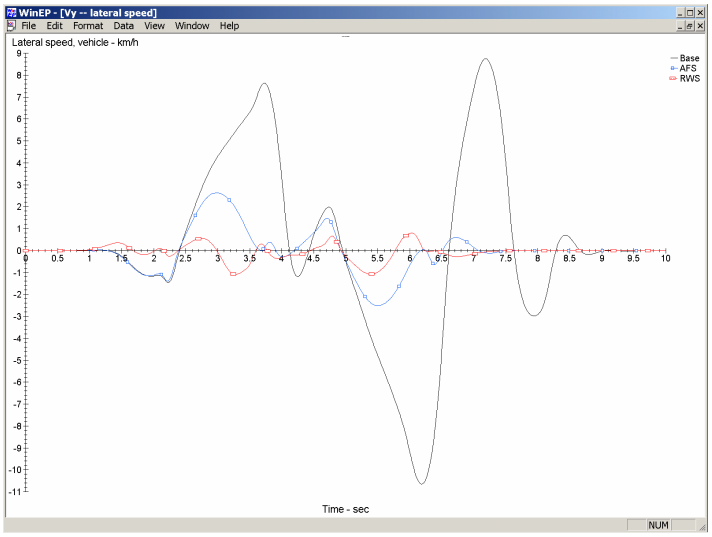

Figure 10: Simulation results for emergency double-lane-change maneuver on snow

Fig. 11 shows the results for a different scenario in which the vehicle, while towing a trailer, is undergoing an emergency lane-change maneuver. (a) shows the side-slip response and (b) shows the hitch angle response. Again, while both AFS and RWS can improve the stability of both the vehicle and the trailer, RWS has much more obvious advantage over AFS in trailering. The trailer exhibits much less swing at the end of the emergency lane-change maneuver using RWS.

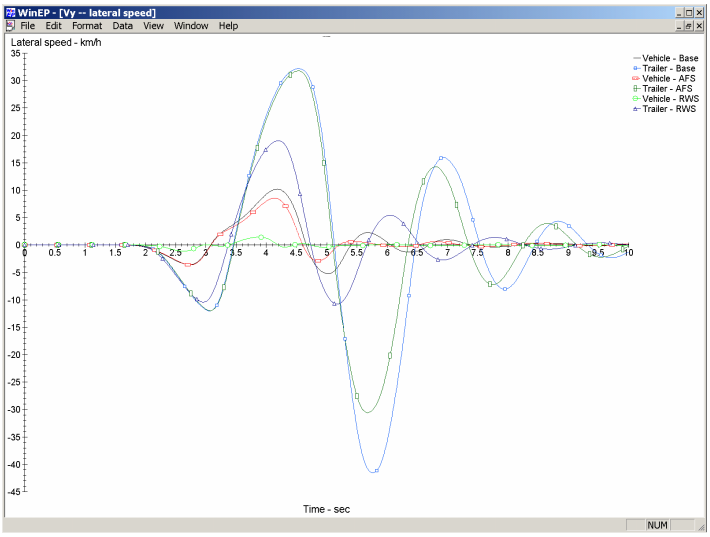

(a). side-slip velocity response

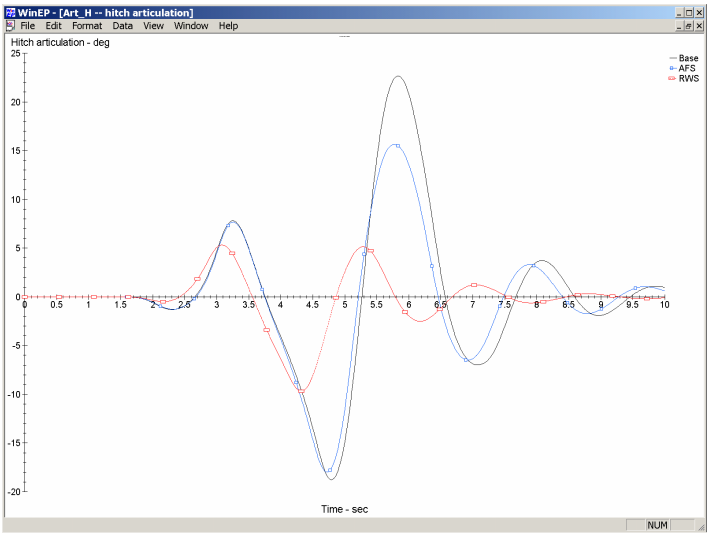

(b). hitch-angle response

Figure 11: Simulation results for emergency lane-change maneuver on wet surface while towing a trailer.

CONCLUSIONS

Using linear analysis, vehicle characteristics under bother front and rear-wheel steering was described by comparing both steady-state and transient responses. Through frequency-domain analysis, a method of designing closed-loop AFS and RWS is developed. Optimization was performed to derive the final closed-loop control gains. Non-linear simulation was lastly performed to verify the analysis results and the control design. It is found that that active steering control can be effective for vehicle stability and handling control. However, while both AFS and RWS can both be used to improve vehicle handling, RWS seems to be better in enhancing the stability through controlling the vehicle side-slip.

REFERENCES

1. Furukawa, Y., Yuhara, N., Sano, S., *et al.*, A review of four-wheel steering studies from the viewpoint of vehicle dynamics and control, Vehicle System Dynamics, Vol. 18, 1989, p. 151-186
2. Akita, R., Present and future of four-wheel-steering technology, SAE:4-13-1-52, JSAE Review, Vol. 13, No. 1, p. 52-57, 1992
3. Furukawa, Y. and Abe, M., Advanced chassis control systems for vehicle handling and active safety, Vehicle System Dynamics, Vol. 28, Nos. 2/3, 1997, p. 59-86
4. Leucht, P.M., Active four-wheel-steering design for the blazer XT-1, SAE Paper No. 872285, 1987
5. Sato, H., Kawai, H. and Isikawa, M., *et al.*, Development for four wheel steering system using yaw-rate feedback control, SAE Paper No. 911922, 1991
6. Vedamuthu, S. and Law, E. H., An investigation of the pulse steer method for determining automobile handling qualities, SAE-930829 (Four parameter evaluation: yaw rate dc-gain, yaw rate Wn and zeta, ay phase lag at 1 Hz)
7. Van Zanten, A. T., Bosch ESP systems: 5 years of experience, SAE-2000-01-1633
8. Ogata, K., Modern Control Engineering, Section 16-2, Prentice-Hall, Inc., Englewood Cliffs, N.J.

APPENDIX:

$$a_{11} = -\frac{C_f + C_r}{Mv_x} \qquad a_{12} = -(\frac{aC_f - bC_r}{Mv_x} + v_x)$$

$$a_{21} = -\frac{aC_f - bC_r}{I_z v_x} \qquad a_{22} = -\frac{a^2 C_f + b^2 C_r}{I_z v_x}$$

$$b_{11} = \frac{C_f}{M} \qquad b_{12} = \frac{C_r}{M}$$

$$b_{21} = \frac{aC_f}{I_z} \qquad b_{22} = -\frac{bC_r}{I_z}$$